

Intramolecular and Intermolecular Hydrogen Bonding in Triphenylphosphine Derivatives of Copper(I) Carboxylates, $(\text{Ph}_3\text{P})_2\text{CuO}_2\text{C}(\text{CH}_2)_n\text{COOH}$. Role of Copper(I) in the Decarboxylation of Malonic Acid and Its Derivatives

Donald J. Darensbourg,* Matthew W. Holtcamp, Bandana Khandelwal, and Joseph H. Reibenspies

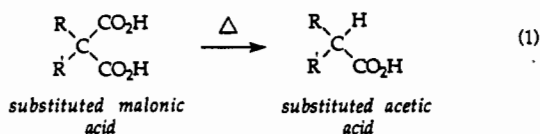
Department of Chemistry, Texas A&M University, College Station, Texas 77843

Received May 12, 1993*

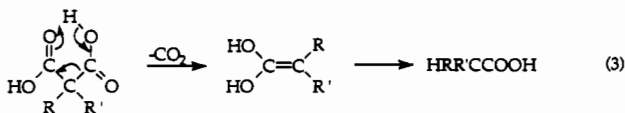
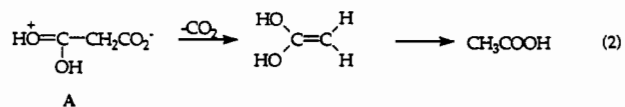
The air-sensitive copper(I) hydrogen dicarboxylate complexes $(\text{Ph}_3\text{P})_2\text{CuO}_2\text{C}(\text{CH}_2)_n\text{COOH}$ ($n = 1, 2$) and derivatives thereof have been synthesized from 1 equiv of the corresponding dicarboxylic acid and cuprous butyrate. The solid-state structures of these derivatives exhibit quite different hydrogen bonding motifs. That is, the malonate derivative (**1**) contains a three-coordinate copper(I) center composed of two phosphine ligands and a monodentate carboxylate ligand. The appended carboxylic acid forms a strong intramolecular hydrogen bond with the distal oxygen atom of the carboxylate group bound to copper. On the other hand, the succinate derivative (**2**) displays a polymeric chain structure in which the carboxylic acid moiety is intermolecularly hydrogen bonded to the neighboring complex. Complex **1** undergoes decarboxylation in tetrahydrofuran solution, whereas complex **2** is stable toward decarboxylation. The phenylmalonic acid analog of complex **1** similarly undergoes carbon dioxide extrusion under milder conditions than **1** and has been shown to proceed *via* a first-order process. This copper(I) derivative is a very effective catalyst for the decarboxylation of phenylmalonic acid to phenylacetic acid and carbon dioxide. This process has been shown to be first-order in copper(I) complex and zero order in [acid]. The rate constants for CO_2 extrusion from the complex and for acid decarboxylation are very similar, an observation consistent with a reaction pathway for the catalytic decarboxylation where the slow step is the extrusion of CO_2 from the half-acid copper(I) complex. The role of intra- and intermolecular hydrogen bonding involving complex **1** on the CO_2 extrusion process is discussed. Crystal data for **1**: space group $P\bar{1}$, $a = 12.949(6)$ Å, $b = 13.162(7)$ Å, $c = 13.253(6)$ Å, $\alpha = 60.73(3)^\circ$, $\beta = 85.26(4)^\circ$, $\gamma = 68.62(4)^\circ$, $Z = 2$, $R = 5.80\%$. Crystal data for **2**: space group $P2_1/n$, $a = 13.141(2)$ Å, $b = 13.0070(10)$ Å, $c = 20.814(3)$ Å, $\beta = 100.300(10)^\circ$, $Z = 4$, $R = 4.00\%$.

Introduction

The thermal instability of malonic acid derivatives toward decarboxylation is well-established.^{1,2} Indeed this process provides a synthetic methodology for the production of monoacids (eq 1).



It has been proposed that intramolecular proton transfer to give the zwitterion (A) plays a significant role in the decarboxylation process (eq 2).³ This is supported by the observations that only



the molecular acid and half-neutralized acid undergo CO_2 loss,

whereas the half-ester monoanion and dianionic salts are stable.⁴ Alternatively a concerted process, where proton transfer is concurrent with carbon–carbon bond fission, as illustrated in eq 3 is plausible.

Importantly, the decarboxylation of malonic diacids has been achieved under mild catalytic conditions using copper(I) reagents.^{5–7} In reactions involving Cu_2O in acetonitrile as catalyst precursor hydrogen dicarboxylates of Cu(I) have been proposed as intermediates in these catalytic processes. Although there is qualitative information about the reaction pathway, a quantitative assessment of the mechanistic aspects of this process is lacking. Relevant to this subject we have found that copper(I) hydrogen dicarboxylates may be prepared from the addition of 1 equiv of dicarboxylic acid to cuprous butyrate. These copper(I) hydrogen dicarboxylates are air-sensitive white solids which are insoluble and/or unstable in a variety of organic solvents; hence, triphenylphosphine was used to stabilize and solubilize these complexes. Previously, copper(I) salts of dicarboxylic acids have been prepared by the reduction of the corresponding copper(II) dicarboxylates with triphenylphosphine.⁸ However, these complexes were reported to be quite insoluble and consequently were only characterized by infrared spectroscopy.

Herein, we report the synthesis of several novel copper(I) carboxylates of the general formula $(\text{Ph}_3\text{P})_2\text{CuO}_2\text{C}(\text{CH}_2)_n\text{CO}_2\text{H}$ ($n = 1, 2$) and derivatives thereof. These derivatives have been characterized by X-ray crystallography at -80°C and by infrared spectroscopy and low-temperature ^1H NMR in solution. Our

* Abstract published in *Advance ACS Abstracts*, December 15, 1993.

(1) Brown, B. R. *Quart. Rev.* **1951**, *5*, 131.
 (2) (a) Carey, F. A.; Sundberg, R. J. *Advanced Organic Chemistry*, 2nd ed.; Plenum Press: New York, 1984; Part B, p 14. (b) March, J. *Advanced Organic Chemistry*, 3rd ed.; Wiley-Interscience: New York, 1985; p 563 and references therein.
 (3) Challis, B. C.; Kerr, S. H.; McDermott, I. R. *J. Chem. Soc., Perkin 2* **1974**, *15*, 1829.

(4) Hall, G. A.; Hanrahan, E. S. *J. Phys. Chem.* **1965**, *69*, 2402.

(5) Toussaint, O.; Capdevielle, P.; Maumy, M. *Tetrahedron* **1984**, *40*, 3229.

(6) Toussaint, O.; Capdevielle, P.; Maumy, M. *Synthesis* **1986**, 1029.

(7) Toussaint, O.; Capdevielle, P.; Maumy, M. *Tetrahedron Lett.* **1987**, *28*, 539.

(8) Hammond, B.; Jardine, F. H.; Vohra, A. G. *J. Inorg. Nucl. Chem.* **1971**, *1017*.

initial investigations assessing the role of copper(I) in the catalytic decarboxylation of malonic acids are presented at this time as well.

Experimental Section

Methods and Materials. All manipulations were carried out under an inert atmosphere unless otherwise stated. The solvents were freshly distilled prior to use. Triphenylphosphine, malonic acid, phenylmalonic acid, succinic acid, butyric anhydride, and butyric acid were purchased from Aldrich Chemical Co. and used as received. Phenylmalonic acid monobenzyl ester was purchased from Lancaster Chemicals. Cuprous butyrate was prepared from the reduction of cupric butyrate by copper turnings in acetonitrile according to published procedures.⁹ Infrared spectra were recorded on a Mattson 6021 spectrometer with DTGS and MCT detectors. ¹H NMR spectra were recorded on a Varian XL-200 superconducting high-resolution spectrometer. Elemental analyses were carried out by Galbraith Laboratories Inc.

Synthesis of (Ph₃P)₂CuO₂CCH₂CO₂H, 1. Cuprous butyrate (0.400 g), malonic acid (0.313 g), and triphenylphosphine (1.40 g) were loaded into a 50-mL flask. Diethyl ether (20 mL) was cannulated into the mixture forming a white slurry. The mixture was stirred for 3 h under argon. The white precipitate which formed was filtered out, washed with approximately 30 mL of diethyl ether, and dried under vacuum. The white powder was recrystallized from dichloromethane yielding 1.48 g (80.9%) of product. Anal. Calcd for C₃₉H₃₃CuO₄P₂: C, 67.77; H, 4.81. Found: C, 67.75; H, 4.98. IR (CH₂Cl₂, cm⁻¹): ν(CO₂) 1592 (s), 1409 (m); ν(CO) 1728 (s).

Recrystallization by slow diffusion of diethyl ether into a dichloromethane solution of **1** produced single, colorless crystals suitable for an X-ray structure analysis.

Synthesis of (Ph₃P)₂CuO₂C(C₂H₄)CO₂H, 2. This compound was prepared in a manner analogous to that of the cuprous malonate monomer described above using cuprous butyrate (0.400 g), succinic acid (0.331 g), and triphenylphosphine (1.40 g). A 1.65-g amount (88.0%) of fine white powder was obtained as product. Anal. Calcd for C₄₀H₃₅CuO₄P₂: C, 68.10; H, 4.97. Found: C, 68.33; H, 5.04. IR (CH₂Cl₂, ν(CO₂), cm⁻¹): 1725 (s), 1549 (s), 1407 (m).

Recrystallization from slow diffusion of diethyl ether into a dichloromethane solution produced single, colorless crystals suitable for an X-ray structure determination.

Synthesis of (Ph₃P)₂CuO₂CCH(C₆H₅)CO₂H, 3. This copper carboxylate was prepared in a manner analogous to that of the cuprous malonate monomer described above using cuprous butyrate (0.400 g), phenylmalonic acid (0.477 g), and triphenylphosphine (1.40 g). A 1.91-g amount (93.6% yield) of a fine white powder was obtained. Anal. Calcd for C₄₅H₃₇CuO₄P₂: C, 70.44; H, 4.86. Found: C, 70.26; H, 3.59. IR (CH₂Cl₂, cm⁻¹): ν(CO₂) 1594 (s), 1384 (m); ν(CO) 1732 (s). On the other hand, if 2 equiv of Cu(I) butyrate is reacted with 1 equiv of phenylmalonic acid, the dimeric bis(triphenylphosphine) copper(I) malonate derivative is formed. This derivative does not undergo decarboxylation.

Synthesis of (Ph₃P)₂CuO₂CCH₂(C₆H₅). (Ph₃P)₂CuO₂CCH(C₆H₅)CO₂H (**3**), 0.432 g, was placed in a 25-mL Schlenk flask under argon. A 10-mL volume of tetrahydrofuran was added to the flask *via* cannula, and the solution was heated to 55.4 °C. Total decarboxylation occurred within 10 min. The reaction was monitored by infrared spectroscopy by following the disappearance of the free acid peak at 1744 cm⁻¹. After the decarboxylation was complete, the solution was cooled to room temperature and allowed to stand overnight in which 0.316 g (83.8% yield) of colorless crystals formed. Anal. Calcd for C₄₄H₃₇CuO₄P₂: C, 73.07; H, 5.16. Found: C, 72.12; H, 4.57. IR (CH₂Cl₂, ν(CO₂), cm⁻¹): 1559 (s), 1395 (m).

Synthesis of (Ph₃P)₂CuO₂CC(C₆H₅)HCO₂CH₂C₆H₅. Cuprous butyrate (0.50 g), phenylmalonic acid monobenzyl ester (1.00 g), and triphenylphosphine (1.76 g) were loaded into a 25-mL Schlenk flask equipped with a stir bar, and the mixture was placed under argon. Diethyl ether, 30 mL, was added *via* syringe, and the resulting slurry was stirred for 3 h in a dry ice-acetone bath. A fine white precipitate formed, which was filtered out, washed with 30 mL of diethyl ether, and dried under vacuum. A 2.2-g amount (78.6% yield) of product was obtained. Anal. Calcd for C₅₂H₄₃CuO₄P₂: C, 72.84; H, 5.05. Found: C, 71.37; H, 5.34. IR (THF, cm⁻¹): ν(CO₂) 1590 (s), 1374 (m); ν(CO) 1740 (s).

Synthesis of (Cy₃P)₂CuO₂CC(C₆H₅)HCO₂H. Cuprous butyrate (0.50 g), phenylmalonic acid (0.610 g), and tricyclohexylphosphine (1.83 g) were reacted in diethyl ether. A 2.32-g amount (86.6% yield) of product

Table 1. Crystallographic Data and Data Collection Parameters

	1	2
formula	C ₄₀ H ₃₅ O ₄ P ₂ Cl ₂ Cu	C ₄₀ H ₃₅ O ₄ P ₂ Cu
fw	776.1	705.2
space group	triclinic, P $\bar{1}$	monoclinic, P ₂ ₁ /n
a, Å	12.949(6)	13.141(2)
b, Å	13.162(7)	13.0070(10)
c, Å	13.253(6)	20.814(3)
α, deg	60.73(3)	
β, deg	85.26(4)	100.300(10)
γ, deg	68.62(4)	
V, Å ³	1822.1(16)	3500.290(0)
Z	2	4
d(calc), g/cm ³	1.414	1.338
abs coeff, mm ⁻¹	0.873	2.051
λ, Å	0.710 73	1.541 78
T, K	193	296
transm coeff	0.7520–0.9427	0.909–0.999
R, %	5.80	4.00
R _w , %	5.40	4.40

^a $R = \sum |F_o - F_c| / \sum F_o$. $R_w = \{[\sum w(F_o - F_c)^2] / [\sum w(F_o)^2]\}^{1/2}$. GOF = 2.65 and 1.42 for complex **1** and **2**, respectively.

was isolated in a manner analogous to that of the previously prepared triphenylphosphine complex. Anal. Calcd for C₄₅H₃₉CuO₄P₂: C, 66.76; H, 9.84. Found: C, 66.62; H, 9.75. IR (THF, cm⁻¹): ν(CO₂) 1600 (s), 1384 (m); ν(CO) 1742 (s).

Decarboxylation Rate of (Ph₃P)₂CuO₂CCH(C₆H₅)CO₂H. The Cu(I) phenylmalonate derivative, 0.400 g, was dissolved in 10 mL of tetrahydrofuran in a 25-mL flask. The flask was equilibrated to 55.4 °C in a thermostated temperature bath (±0.1 °C). The disappearance in the infrared of the carboxylate stretch at 1744 cm⁻¹ (THF) was monitored *vs* time. A plot of the absorbance of the free acid peak *vs* time was exponential. Rate constants were determined from the slope of the ln(A) *vs* time plot. Decarboxylation rates were also obtained at 20 and 30 °C for the analogous tricyclohexylphosphine complex. No decarboxylation was observed under similar conditions using the solvent, dichloromethane (ν(CO) 1728 cm⁻¹).

Decarboxylation of Phenylmalonic Acid. Phenylmalonic acid, 0.225 g, and tricyclohexylphosphine cuprous hydrogen phenylmalonate, 0.05 g, were weighed into separate 25-mL flasks. A 5-mL volume of tetrahydrofuran was syringed into each flask. Both flasks were warmed to 55.4 °C with subsequent transfer of the acid solution *via* cannula into the catalyst-containing flask. Infrared spectra were obtained every 5–10 min. A plot of A/A⁰ for the acid *vs* time was linear indicating zero-order dependence in acid. Upon doubling of the concentration of copper(I) complex, the rate constant for acid decarboxylation was doubled, indicative of first-order behavior in [catalyst]. When phenylmalonic acid was heated in THF at 55.4 °C in the *absence* of a Cu(I) catalyst for a period greater than 1 h, *no* decarboxylation was observed.

Attempted Decarboxylation of (Ph₃P)₂CuO₂C(C₆H₅)HCO₂-(C₂H₅)₄N⁺. One equivalent of tetraethylammonium hydroxide, (25% w/w solution in methanol) was added to (Ph₃P)₂CuO₂CCH(C₆H₅)CO₂H, 0.200 g. The complex was dissolved in 20 mL of tetrahydrofuran. The solvent mixture was removed by vacuum. A 10-mL volume of tetrahydrofuran was added *via* cannula, and the solution was placed in a 55.4 °C water bath. Monitoring by IR spectroscopy indicated total deprotonation of the complex: ν(CO₂) (cm⁻¹, THF) 1622 (s), 1591 (s), 1378 (m). After 30 min of heating, *no* decarboxylation occurred.

X-ray Crystal Data for 1 (C₄₀H₃₅O₄P₂Cl₂Cu). A colorless plate (0.05 mm × 0.22 mm × 0.24 mm) was mounted on a glass fiber with epoxy cement at room temperature and cooled to 193 K in a N₂ cold stream. Data are as follows: $M_r = 776.1$; space group P $\bar{1}$; $a = 12.949(6)$, $b = 13.162(7)$, $c = 13.253(6)$ Å; $\alpha = 60.73(3)$, $\beta = 85.26(4)$, $\gamma = 68.62(4)$ °; $V = 1822.1(16)$ Å³, $D_{\text{calc}} = 1.414$ g cm⁻³, $Z = 2$; Siemens R3m/V X-ray diffractometer; 193 K; Mo K α ($\lambda = 0.710 73$ Å); scan method ω (Wyckoff); data collection range $4.0^\circ \leq 2\theta \leq 50^\circ$; number of unique data 3594; number of total data used 2665 ($I \geq 2.0\sigma(I)$); solved by direct methods with full-matrix least-squares anisotropic refinement for all non-hydrogen atoms (number of least-squares parameters = 443); $R = 0.058$, $R_w = 0.054$, $S = 2.65$. Crystal data and experimental conditions are provided in Table 1.

X-ray Crystal Data for 2 (C₄₀H₃₅O₄P₂Cu). A colorless plate (0.11 mm × 0.44 mm × 0.42 mm) was mounted on a glass fiber with epoxy cement at room temperature. Data are as follows: $M_r = 705.2$; space group P₂₁/n (No. 14, a nonstandard setting for the space group P₂₁/c); $a = 13.141(2)$, $b = 13.0070(10)$, $c = 20.814(3)$ Å; $\beta = 100.300(10)$ °;

(9) Edwards, D. A.; Richards, R. *J. Chem. Soc., Dalton Trans.* 1973, 2463.

Table 2. Atomic Coordinates ($\times 10^4$) and Equivalent Isotropic Displacement Parameters ($\text{\AA}^2 \times 10^3$) for Complex 1

	x	y	z	$U(\text{eq})^{a,b}$
Cu(1)	2294(1)	8624(1)	8702(1)	35(1)
Cl(1)	-651(3)	6613(3)	5640(3)	103(2)
Cl(2)	1415(3)	6927(4)	5559(4)	174(3)
P(1)	3294(2)	9187(2)	7198(2)	33(1)
P(2)	2498(2)	8371(2)	10490(2)	31(1)
O(1)	822(5)	8547(6)	8295(5)	41(4)
O(2)	2095(5)	6652(6)	8997(5)	51(4)
O(3)	1639(6)	4935(6)	9059(6)	71(5)
O(4)	-90(5)	5250(6)	8602(5)	59(5)
C(1)	1111(8)	7423(10)	8598(7)	34(6)
C(2)	225(7)	6942(8)	8527(8)	46(6)
C(3)	562(9)	5639(9)	8728(8)	42(7)
C(4)	3367(7)	11117(9)	7473(8)	38(6)
C(5)	3418(7)	12274(10)	7130(9)	45(7)
C(6)	3449(7)	13079(9)	5966(9)	47(7)
C(7)	3414(7)	12704(9)	5178(8)	48(7)
C(8)	3370(7)	11541(9)	5511(8)	44(6)
C(9)	3345(6)	10723(8)	6682(8)	31(6)
C(10)	1760(8)	9868(9)	5428(8)	45(7)
C(11)	1387(8)	10027(9)	4398(8)	54(7)
C(12)	2160(10)	9529(10)	3802(8)	55(7)
C(13)	3255(9)	8896(9)	4246(8)	51(7)
C(14)	3620(7)	8758(8)	5270(8)	42(6)
C(15)	2865(7)	9272(8)	5881(7)	32(5)
C(16)	5643(8)	8526(9)	7209(7)	40(6)
C(17)	6725(8)	7660(10)	7511(8)	42(6)
C(18)	6947(8)	6395(10)	8156(8)	52(7)
C(19)	6079(9)	5971(9)	8513(8)	53(7)
C(20)	5001(8)	6834(9)	8222(8)	44(7)
C(21)	4745(7)	8125(8)	7562(7)	32(6)
C(22)	1803(7)	10863(9)	9946(7)	35(6)
C(23)	1913(7)	11918(9)	9827(7)	39(6)
C(24)	2906(8)	11802(9)	10278(8)	42(7)
C(25)	3758(8)	10643(10)	10824(8)	46(7)
C(26)	3641(7)	9565(8)	10965(7)	38(6)
C(27)	2659(7)	9672(8)	10512(7)	27(5)
C(28)	725(7)	7669(8)	11857(7)	35(6)
C(29)	-77(7)	8377(9)	12573(8)	46(7)
C(30)	-231(7)	7331(10)	12751(8)	45(7)
C(31)	376(7)	6635(9)	12245(8)	43(6)
C(32)	1179(7)	7004(8)	11535(7)	34(6)
C(33)	1356(6)	8047(8)	11373(7)	30(5)
C(34)	3739(8)	6346(9)	12625(9)	52(7)
C(35)	4697(10)	5343(10)	13321(9)	61(7)
C(36)	5658(9)	5025(10)	12817(12)	70(8)
C(37)	5631(9)	5757(11)	11620(11)	66(8)
C(38)	4694(8)	6729(9)	10945(9)	48(6)
C(39)	3704(7)	7038(8)	11438(8)	35(6)
C(40)	839(8)	5798(10)	5809(9)	99(9)

^a Equivalent isotropic U defined as one-third of the trace of the orthogonalized U_{ij} tensor. ^b Estimated standard deviations are given in parentheses.

$V = 3500.290(0) \text{ \AA}^3$; $Z = 4$; $d_{\text{calc}} = 1.338 \text{ g cm}^{-3}$; Rigaku AFC5R X-ray diffractometer (Cu $K\alpha$ $\lambda = 1.54178 \text{ \AA}$); scan method ω (Wyckoff); data were collected for $5.0^\circ \leq 2\theta \leq 120.0^\circ$; number of unique data 5759; number of total data used 3779 ($I \geq 2\sigma(I)$); solved by direct methods with full-matrix least-squares squares parameters = 428; $R = 0.040$, $R_w = 0.044$, $S = 1.42$. Crystal data and experimental conditions are provided in Table 1.

Results and Discussion

The solid-state structure of $(\text{Ph}_3\text{P})_2\text{Cu}(\text{O}_2\text{CCH}_2\text{CO}_2\text{H})$ (**1**) has been determined in order to provide a definitive description of the binding of the carboxylate functionality to the metal center. Slow diffusion of diethyl ether into a CH_2Cl_2 solution of complex **1** afforded crystals which were suitable for a single-crystal X-ray diffraction investigation. The final atomic positional and equivalent isotropic displacement parameters are listed in Table 2. Selected interatomic distances and angles are given in Table 3. Figure 1 depicts the structure of complex **1**, which is monomeric with intramolecular hydrogen bonding. One molecule of CH_2Cl_2 crystallized per copper(I) complex in the unit cell. The Cu(1)–O(1) distance at 2.073(7) \AA is indicative of strong bonding,

Table 3. Selected Bond Lengths (\AA) and Bond Angles (deg) for Complex 1^a

Cu(1)–P(1)	2.244(3)	Cu(1)–P(2)	2.249(3)
Cu(1)–O(1)	2.073(7)	Cu(1)–O(2)	2.536(9)
Cu(1)–C(1)	2.62(1)	P(1)–C(9)	1.82(1)
P(1)–C(15)	1.82(1)	P(1)–C(21)	1.815(8)
P(2)–C(27)	1.81(1)	P(2)–C(33)	1.850(9)
P(2)–C(39)	1.808(7)	O(1)–C(1)	1.24(1)
O(2)–C(1)	1.26(1)	O(3)–C(3)	1.33(1)
O(4)–C(3)	1.20(2)	C(1)–C(2)	1.53(2)
C(2)–C(3)	1.49(2)		
P(1)–Cu(1)–P(2)	131.1(1)	P(1)–Cu(1)–O(1)	113.7(2)
P(2)–Cu(1)–O(1)	114.6(2)	P(1)–Cu(1)–O(2)	106.1(2)
P(2)–Cu(1)–O(2)	106.4(2)	P(1)–Cu(1)–C(1)	113.2(2)
P(2)–Cu(1)–C(1)	112.8(2)	Cu(1)–P(1)–C(9)	113.4(3)
Cu(1)–P(1)–C(15)	117.9(3)	Cu(1)–P(2)–C(27)	114.9(3)
Cu(1)–P(1)–C(21)	112.6(3)	Cu(1)–O(1)–C(1)	101.8(6)
Cu(1)–P(2)–C(33)	114.3(4)	Cu(1)–C(1)–O(2)	72.1(7)
Cu(1)–P(2)–C(39)	114.9(4)	Cu(1)–C(1)–C(2)	168.7(7)
Cu(1)–O(2)–C(1)	79.7(7)	O(2)–C(1)–C(2)	119.0(1)
O(1)–C(1)–O(2)	123.0(1)	O(3)–C(3)–O(4)	122.0(1)
O(1)–C(1)–C(2)	118.6(7)	O(4)–C(3)–C(2)	122.6(8)
C(1)–C(2)–C(3)	120.1(8)	O(3)–C(3)–C(2)	116(1)

^a Estimated standard deviations are given in parentheses.

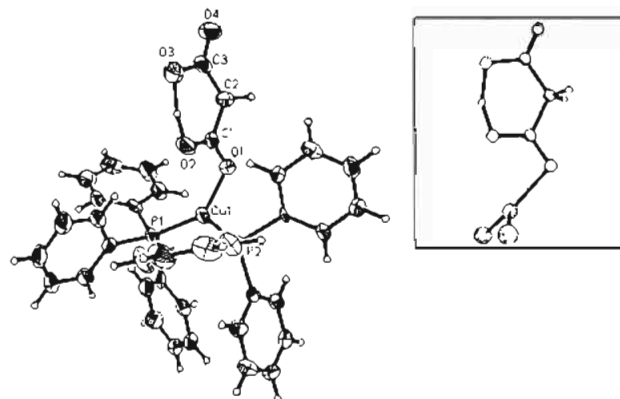


Figure 1. Molecular structure of $\text{Cu}(\text{O}_2\text{CCH}_2\text{CO}_2\text{H})(\text{P}(\text{C}_6\text{H}_5)_3)_2$ (**1**), with thermal ellipsoids drawn at the 50% probability level. The hydrogen-bonding motif is schematically represented in the boxed drawing, where the phosphine phenyl rings are omitted.

and the Cu(1)–O(2) distance at 2.536(9) \AA indicates a very weak interaction. The mono-protonated dicarboxylic acid function forms a six-membered ring (deviation from planarity, $\pm 0.0295 \text{ \AA}$) in which the hydrogen was located between the O(2) and O(3) atoms which are separated by 2.500 \AA , indicative of a strong *intramolecular* hydrogen-bonding interaction. The O(3) and O(4) of the neighboring molecule distance of 3.504 \AA clearly illustrates the lack of *intermolecular* hydrogen bonding between the monomeric units.

Intramolecular hydrogen bonding has been observed in several mono-protonated dicarboxylate anions.¹⁰ For example, *intramolecular* hydrogen bonding is seen in potassium hydrogen maleate where the oxygen atoms of the two carboxylate functions are chelated *via* strong hydrogen bonding with an oxygen–oxygen distance of 2.44 \AA .¹¹ On the other hand, potassium hydrogen malonate exhibits *intermolecular* hydrogen bonding, forming an “infinite ribbon structure”.¹² Hence, it is interesting that complex **1** adopts a structure with intramolecular hydrogen bonding as in potassium hydrogen maleate rather than intermolecular as in hydrogen malonate.

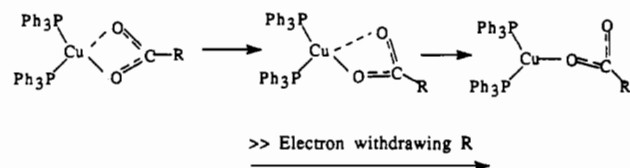
This complex represents the first crystallography characterized trigonal planar Cu(I) carboxylate. The Cu(1)–P(1) and Cu(1)–P(2) bond distances are 2.244 and 2.249 \AA , respectively. The

(10) (a) Speakman, J. C. *Struct. Bonding (Berlin)* 1972, 12, 141. (b) Emsley, J. *Chem. Soc. Rev.* 1980, 9, 91.

(11) Darlow, S. F.; Cochran, W. *Acta Crystallogr.* 1961, 14, 1250.

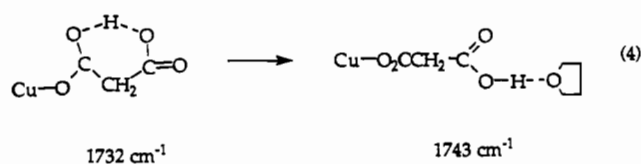
(12) Sime, J. G.; Speakman, J. C.; Parthasarathy, R. *J. Chem. Soc. A* 1970, 1919.

corresponding P(1)–Cu(1)–P(2) bond angle is 131.1°. This obtuse angle is typical for (triphenylphosphine) copper(I) complexes and reflects the steric requirements of the triphenylphosphine ligand.¹³ Distorted tetrahedral Cu(I) triphenylphosphine complexes have P–Cu–P bond angles ranging from 120 to 133°. ^{14,15} It has been reported that the P–Cu–P bond angle decreases as the nonplanarity and size of the anion increases; therefore, the largest bond angles would be anticipated for small planar chelating anions.¹⁵ The carboxylate is best considered monodentate, since the Cu(1)–O(2) distance is 2.5 Å, which is nonbonding or very weak. This weak interaction of O(2) with copper(I) distorts the trigonal planar structure slightly with the deviation of the P(1), Cu(1), P(2), O(1) plane from planarity, being only ±0.034 Å. It might be expected that increasing the basicity of the carboxylate would strengthen the interaction between O(2) and the Cu(1) center; therefore, carboxylates of higher basicity would be predicted to have tetrahedral structures and carboxylates of lower basicity would favor three-coordinate trigonal planar complexes. Indeed, the crystal structure of (triphenylphosphine) copper(I) acetate (a more basic carboxylate in comparison to malonate) is reported to be a distorted tetrahedral complex with asymmetric bond lengths of 2.162 and 2.257 Å.^{14,16,17} The asymmetry is expected to decrease as the basicity of the carboxylate increases. Hammond *et al.*⁸ noted from observed infrared stretching frequencies for the bound carboxylate ligand that acids with a low pK_a generally gave monodentate structures while acids with a high pK_a gave either monodentate or bidentate structures. Further studies in our laboratories are currently being undertaken to determine the generality of the proposed trend based on X-ray structural data.



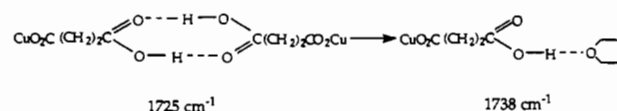
In a methylene chloride solution complex **1** displayed infrared bands at 1732 (m), 1592 (m), and 1409 (m) cm^{-1} . The peak at 1732 cm^{-1} is assigned to the asymmetric $\nu(\text{C}=\text{O})$ stretch, whereas the peaks at 1592 and 1409 cm^{-1} correspond to the asymmetric and symmetric $\nu(\text{CO}_2)$ frequencies of the copper bound carboxylate. The large difference in $\nu(\text{CO}_2)$ frequencies ($\Delta = 183 \text{ cm}^{-1}$) is indicative of a monodentate structure in solution as well. The proton was located by ^1H NMR in CD_3Cl at -90°C at 15.6 ppm, shifting to 16.1 ppm upon dilution. The malonate's $-\text{CH}_2$ unit has a proton resonance at 3.1 ppm. The $\nu(\text{COOH})$ band for complex **1** is shifted to higher frequency, at 1743 cm^{-1} , in tetrahydrofuran solution, which is indicative of intermolecular hydrogen bonding with the more polar solvent (eq 4). On the other hand, the asymmetric and symmetric $\nu(\text{CO}_2)$ vibrations observed at 1591 and 1409 cm^{-1} in THF are essentially unperturbed by the solvent change.

Single crystals of the succinate derivative, $(\text{Ph}_3\text{P})_2\text{CuO}_2\text{C}(\text{CH}_2)_2\text{COOH}$ (**2**), were obtained in the same manner as those



of complex **1**. The final atomic positional and equivalent isotropic displacement parameters are listed in Table 4. Selected interatomic distances and angles are given in Table 5. X-ray crystallography has revealed a novel type of *intermolecular* hydrogen bonding for this complex as is illustrated in Figure 2. Complex **2** crystallized in a polymeric chain structure in which the carboxylic acid moiety is hydrogen bonded to the neighboring complex in a new hydrogen-bonding fashion. That is, a six-membered ring is formed with the $-\text{COOH}$ moiety and Cu(1a)–O(1a) unit, with a derivation from ring planarity of ± 0.01 Å. The Cu(1)–O(1) bond distance at 2.051(3) Å is indicative of a strong interaction, whereas the Cu(1a)–O(3) distance of 2.368(3) Å indicates a weak interaction. The O(1a)–O(4) distance of 2.517 Å is typical for strong hydrogen bonding and is probably a key interaction in forming the six-membered ring. The potassium salt of hydrogen succinate has been found to crystallize with intermolecular hydrogen bonding similar to that of potassium hydrogen malonate discussed earlier.¹² The succinate complex has Cu(1)–P(1) and Cu(1)–P(2) bond distances of 2.250 and 2.232 Å, with a P(1)–Cu(1)–P(2) angle of 129.1°. These values are very similar to other reported Cu(I) triphenylphosphine structures. The ketonic oxygen, O(3a), of the nearest neighbor was found bound to Cu(1) with a 2.368-Å bond distance. This weak bond distorts the complex's trigonal planar geometry of the P(1), Cu(1), P(2), O(1) atoms (deviation from planarity, ± 0.055 Å). The increased deviation from planarity, as compared to the trigonal planar malonate complex, is expected due to the stronger Cu(1)–O(3a) interaction. Hence, in this instance the Cu(I) center is best described as possessing a highly distorted tetrahedron geometry in the solid state.

The solid-state infrared spectrum of **2** in the $\nu(\text{COOH})$ region exhibits a $\nu(\text{C}=\text{O})$ vibration at 1682 cm^{-1} , indicative of the interaction of the ketonic oxygen of the acid moiety with the neighboring Cu(I) center as depicted in Figure 2. The monodentate bound carboxylate displays an asymmetric stretch at 1636 cm^{-1} and symmetric stretch at 1330 cm^{-1} ($\Delta\nu = 306 \text{ cm}^{-1}$). The polymeric structure of complex **2** breaks down in solution. That is, the infrared spectrum of $(\text{Ph}_3\text{P})_2\text{Cu}(\text{O}_2\text{C}(\text{CH}_2)_2\text{CO}_2\text{H})$ in dichloromethane displayed a $\nu(\text{C}=\text{O})$ asymmetric stretch at 1725 cm^{-1} with $\nu(\text{CO}_2)$ asymmetric and symmetric stretches at 1548 and 1408 cm^{-1} . The shift of the $\nu(\text{C}=\text{O})$ to 1725 cm^{-1} is indicative



of dimer formation in solution *via* intermolecular hydrogen bonding. On the other hand, in tetrahydrofuran, the complex hydrogen bonds to the solvent as indicated by the shift of the asymmetric stretch to 1738 cm^{-1} . The asymmetric and the symmetric $\nu(\text{CO}_2)$ frequencies were assigned to the peaks at 1548 and 1408 cm^{-1} , respectively.¹⁸ The difference between the asymmetric and the symmetric $\nu(\text{CO}_2)$ ($\Delta = 140 \text{ cm}^{-1}$) is typical of a chelated carboxylate. Low-temperature ^1H -NMR located a very broad peak at 15.7 ppm at -60°C . Dilution of the sample resulted in a shift to 16.1 ppm verifying that the proton had been located. The $-\text{CH}_2$ moiety of succinate was located at 2.2 ppm, which broadens at -80°C and separates into two broad separate

- (13) (a) Tolman, C. A. *Chem. Rev.* **1977**, *77*, 313. (b) Brown, T. L. *Inorg. Chem.* **1992**, *31*, 1286.
 (14) Drew, M. G. B.; Othman, A. H.; Edwards, D. A.; Richards, R. *Acta Crystallogr., Sect. B* **1975**, *B31*, 2695.
 (15) (a) Messner, G. G.; Palenik, G. J. *Inorg. Chem.* **1969**, *8*, 2750. (b) Lippard, S. J.; Melmed, K. M. *Inorg. Chem.* **1969**, *8*, 2775. (c) Lippard, S. J.; Melmed, K. M. *Inorg. Chem.* **1967**, *6*, 2223. (d) Corfield, P. W. R.; Shearer, H. M. M. *Acta Crystallogr.* **1966**, *21*, 957. (e) Camus, A.; Marisch, N.; Nardin, G.; Randaccio, L. *J. Chem. Soc., Dalton Trans.* **1975**, 2560. (f) Marsich, N.; Camus, A.; Nardin, G. *J. Organomet. Chem.* **1982**, *239*, 429.
 (16) $(\text{Ph}_3\text{P})_2\text{CuO}_2\text{CCH}_3$ has been structurally characterized at ambient temperature¹⁴ and -80°C ¹⁷ and found to contain a chelating carboxylate ligand. In addition, on the basis of $\nu(\text{CO}_2)$ infrared measurements, we find this geometry to exist as well in solution.
 (17) Darensbourg, D. J.; Longridge, E. M.; Reibenspies, J. H. Unpublished results.

- (18) The $\nu(\text{CO}_2)$ frequencies were unambiguously identified by preparing the Cu(I) hydrogen adipate complex, from ^{13}C -labeled adipic acid. $\nu(^{13}\text{CO}_2)$ frequencies are given following unlabeled values: 1730 (m), 1546 (s), and 1410 (m) cm^{-1} ; 1684 (m), 1508 (s), and 1388 (m) cm^{-1} .

Table 4. Atomic Coordinates ($\times 10^4$) and Equivalent Isotropic Displacements Parameters ($\text{\AA}^2 \times 10^3$) for Complex **2**

	x	y	z	$U(\text{eq})^{a,b}$
Cu(1)	1596(1)	1945(1)	8802(1)	47(1)
P(1)	-31(1)	1897(1)	8236(1)	44(1)
P(2)	2225(1)	2817(1)	9710(1)	42(1)
O(1)	2548(2)	812(2)	8563(1)	52(1)
O(2)	1743(3)	-458(2)	8950(2)	110(2)
O(3)	2755(2)	-2127(2)	7017(1)	64(1)
O(4)	1707(3)	-3286(2)	7317(2)	79(1)
C(1)	2261(3)	-124(3)	8572(2)	58(2)
C(2)	2589(3)	-827(3)	8062(2)	62(2)
C(3)	1900(4)	-1736(3)	7899(2)	74(2)
C(4)	2164(3)	-2397(3)	7365(2)	53(1)
C(5)	471(3)	816(4)	7185(2)	74(2)
C(6)	313(4)	141(4)	6670(2)	92(2)
C(7)	-612(4)	-361(4)	6502(2)	83(2)
C(8)	-1377(4)	-178(3)	6848(3)	77(2)
C(9)	-1229(3)	501(3)	7362(2)	63(2)
C(10)	-300(3)	1020(3)	7541(2)	47(1)
C(11)	-2021(3)	2074(3)	8582(2)	60(2)
C(12)	-2767(3)	1769(4)	8937(2)	74(2)
C(13)	-2567(4)	997(4)	9379(2)	79(2)
C(14)	-1632(4)	499(4)	9481(2)	78(2)
C(15)	-882(3)	793(3)	9131(2)	60(2)
C(16)	-1066(3)	1588(3)	8683(2)	46(1)
C(17)	-502(3)	3400(4)	7243(2)	75(2)
C(18)	-693(5)	4398(5)	7033(3)	107(3)
C(19)	-739(4)	5176(4)	7467(3)	102(3)
C(20)	-588(4)	4974(4)	8121(3)	91(2)
C(21)	-391(3)	3975(3)	8335(2)	71(2)
C(22)	-363(3)	3173(3)	7900(2)	52(1)
C(23)	2309(3)	2535(4)	11062(2)	79(2)
C(24)	1884(4)	2265(5)	11597(2)	100(2)
C(25)	886(4)	1930(4)	11525(2)	80(2)
C(26)	293(3)	1888(3)	10923(2)	69(2)
C(27)	706(3)	2165(3)	10382(2)	58(1)
C(28)	1726(3)	2485(3)	10445(2)	46(1)
C(29)	4326(3)	3429(3)	10060(2)	74(2)
C(30)	5370(3)	3239(4)	10249(3)	88(2)
C(31)	5713(3)	2271(4)	10360(2)	72(2)
C(32)	5040(3)	1475(4)	10272(3)	90(2)
C(33)	3992(3)	1664(3)	10060(2)	80(2)
C(34)	3620(3)	2648(3)	9967(2)	44(1)
C(35)	1903(4)	4816(3)	10158(2)	77(2)
C(36)	1782(4)	5874(4)	10079(3)	91(2)
C(37)	1795(3)	6312(3)	9489(3)	75(2)
C(38)	1944(3)	5719(3)	8983(2)	74(2)
C(39)	2066(3)	4666(3)	9054(2)	62(2)
C(40)	2052(3)	4202(3)	9647(2)	46(1)

^a Equivalent isotropic U defined as one-third of the trace of the orthogonalized U_{ij} tensor. ^b Estimated standard deviations are given in parentheses.

Table 5. Selected Bond Lengths (\AA) and Bond Angles (deg) for Complex **2**^a

Cu(1)-P(1)	2.250(1)	Cu(1)-P(2)	2.232(1)
Cu(1)-O(1)	2.051(3)	Cu(1)-O(3A)	2.368(3)
O(1)-C(1)	1.276(5)	O(2)-C(1)	1.210(6)
O(3)-C(4)	1.206(5)	O(3)-Cu(1A)	2.368(3)
O(4)-C(4)	1.298(5)	C(1)-C(2)	1.519(6)
C(2)-C(3)	1.492(6)	C(3)-C(4)	1.494(6)
P(1)-Cu(1)-P(2)	129.1(1)	P(1)-Cu(1)-O(1)	114.6(1)
P(2)-Cu(1)-O(1)	114.8(1)	P(1)-Cu(1)-O(3A)	93.9(1)
P(2)-Cu(1)-O(3A)	102.9(1)	O(1)-Cu(1)-O(3A)	83.0(1)
Cu(1)-P(1)-C(10)	117.6(1)	Cu(1)-P(1)-C(16)	117.6(1)
Cu(1)-P(2)-C(28)	117.1(1)	Cu(1)-P(2)-C(22)	108.4(1)
Cu(1)-O(1)-C(1)	119.2(3)	Cu(1)-P(2)-C(34)	112.8(1)
O(1)-C(1)-O(2)	123.5(4)	Cu(1)-P(2)-C(40)	114.9(1)
O(2)-C(1)-C(2)	120.1(4)	C(4)-O(3)-Cu(1A)	129.6(2)
C(2)-C(3)-C(4)	114.4(4)	O(1)-C(1)-C(2)	116.3(4)
O(3)-C(4)-C(3)	122.6(4)	C(1)-C(2)-C(3)	113.5(4)
O(4)-C(4)-C(3)	113.8(4)	O(3)-C(4)-O(4)	123.6(4)

^a Estimated standard deviations are given in parentheses.

peaks at 2.5 and 2.2 ppm at -90°C indicating slight inequivalence at these low temperatures. We have found that copper(I) hydrogen glutarate and adipate complexes have infrared $\nu(\text{CO}_2)$

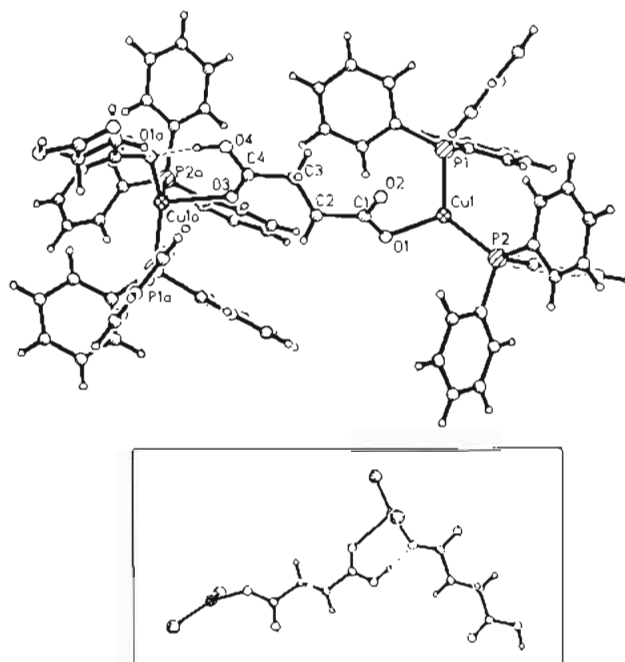
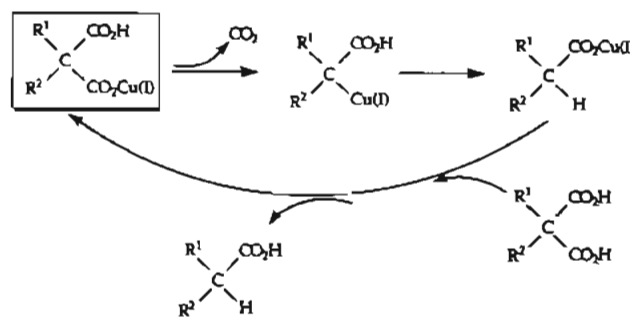
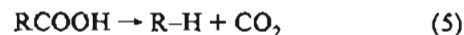


Figure 2. Molecular structure and atomic labels of $\text{Cu}(\text{O}_2\text{CCH}_2\text{CH}_2\text{CO}_2\text{H})[\text{P}(\text{C}_6\text{H}_5)_3]_2$ (**2**). The hydrogen-bonding motif is schematically represented in the boxed drawing, where the phosphine phenyl rings are omitted.

Scheme 1

frequencies in dichloromethane similar to that of the succinate derivative. Hence, it is probable that these complexes exhibit an hydrogen-bonding motif similar to that observation for the succinate complex dissolved in dichloromethane.

The intermediacy of complexes of the general structure of **1** has been proposed in the Cu_2O -catalyzed production of monocarboxylic acids from malonic acids as indicated in Scheme 1. It is of importance to note that the decarboxylation step, which proceeds *via* an ionic mechanism, is enhanced by the presence of at least one electron-withdrawing and/or resonance-stabilized R substituent on the malonic acid.^{5,19,20} That is, in general carboxylic acids which most easily undergo the decarboxylation reaction (eq 5) contain electron-withdrawing R substituents (large, positive



Taft σ values, σ^*), e.g., cyanoacetic acid, NCCH_2COOH ($\sigma^* = 1.30$). Consistent with this the monocarboxylate complex derived from $\text{HOOCCH}_2\text{COOH}$ ($\sigma^* = 1.10$), complex **1**, undergoes decarboxylation to provide $(\text{Ph}_3\text{P})_2\text{CuO}_2\text{CCH}_3$ in refluxing DME,²¹ whereas the analogous complex **2** derived from

(19) This process is to be contrasted with the higher temperature oxidative decarboxylation of carboxylate derivatives of Ph_3PAu^+ .²⁰

(20) Fackler, J. P., Jr.; Khan, Md. N. I.; King, C.; Staples, R. J.; Winpenny, R. E. P. *Organometallics* 1991, 10, 2178.

(21) This reaction occurs slowly in refluxing DME with a half-life of several hours.

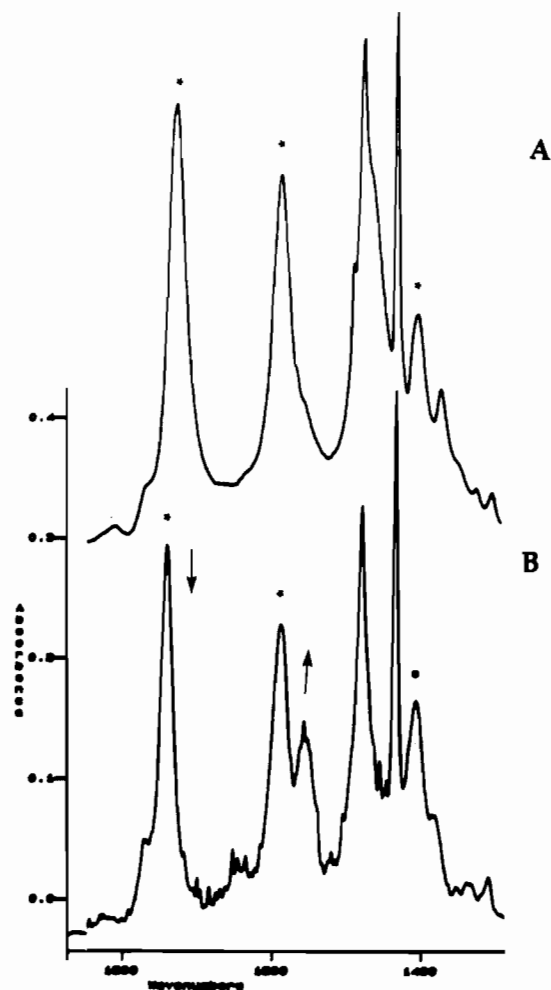
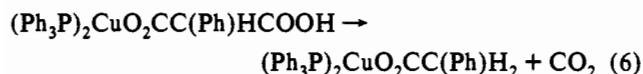


Figure 3. Infrared spectra of complex 1: (A) in methylene chloride with peaks marked by asterisks corresponding to $\nu(\text{COOH})$, 1732 cm^{-1} , and $\nu(\text{CO}_2)_{\text{asym}}$ and $\nu(\text{CO}_2)_{\text{sym}}$ at 1592 and 1409 cm^{-1} , respectively; (B) in tetrahydrofuran with analogous peaks at 1743 , 1591 , and 1409 cm^{-1} , respectively. Peaks used to monitor diacid disappearance and monoacid appearance are marked by \downarrow and \uparrow , respectively.

$\text{HOOCCH}_2\text{CH}_2\text{COOH}$ ($\sigma^* = 0.35$) does not undergo decarboxylation under similar conditions.

Well-characterized copper(I) malonate derivatives, such as complex 1, have allowed us to investigate the mechanistic aspects of this important catalytic decarboxylation process. Although complex 1 undergoes decarboxylation, it was advantageous to study the phenylmalonate derivative (eq 6) since it undergoes carbon dioxide extrusion under milder reaction conditions.



Reaction 6 was monitored in THF by following the $\nu(\text{C}=\text{O})$ vibration of the $-\text{COOH}$ functionality in 3 in the infrared at 1743 cm^{-1} (Figure 3). The reaction was found to be first order in [3] as indicated by a linear plot of $\ln[3]$ vs time (Figure 4). Furthermore, the decarboxylation reaction was retarded when carried out in an atmosphere of carbon dioxide (Figure 5). That is, the first-order rate constant for CO_2 loss was $3.75 \times 10^{-3}\text{ s}^{-1}$ at $55.4\text{ }^\circ\text{C}$ in an argon atmosphere compared to $2.42 \times 10^{-3}\text{ s}^{-1}$ in a carbon dioxide atmosphere (CO_2 solubility in THF at $55.4\text{ }^\circ\text{C}$ is 0.24 M). Of significance to the mechanistic details of this process, when a $>90\%$ ^{13}C -labeled carbon dioxide atmosphere was employed, *no* ^{13}C -label was observed in the acid function of complex 3, with some ^{13}C enrichment being noted in the carboxylate moiety.

Upon replacement of the triphenylphosphine ligands in complex 3 with the more electron-donating and sterically encumbering

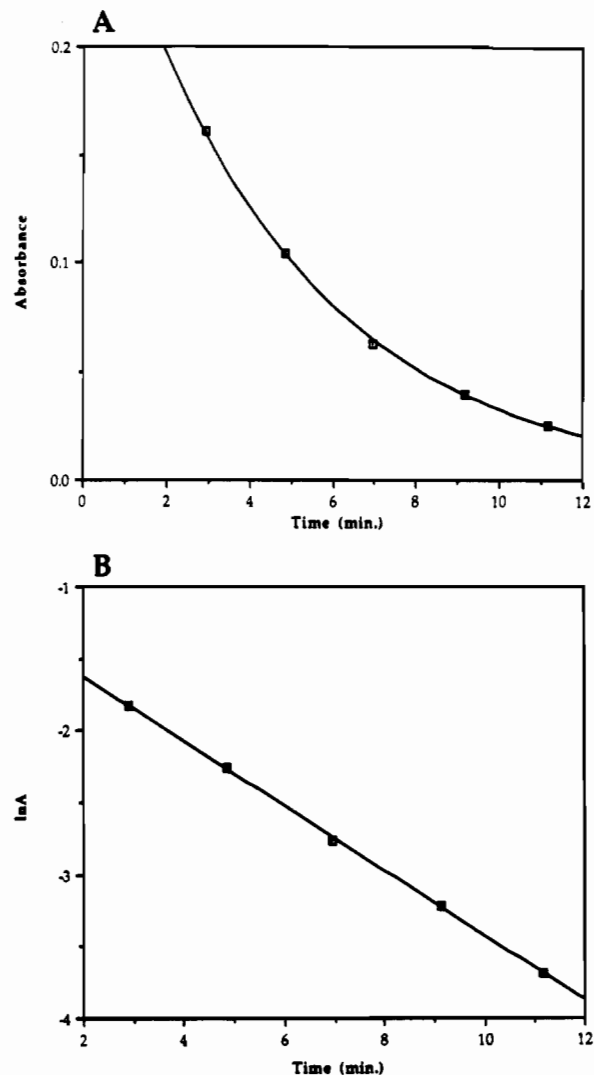


Figure 4. First-order dependence of CO_2 extrusion from complex 3 on [3] in THF at $55.4\text{ }^\circ\text{C}$.

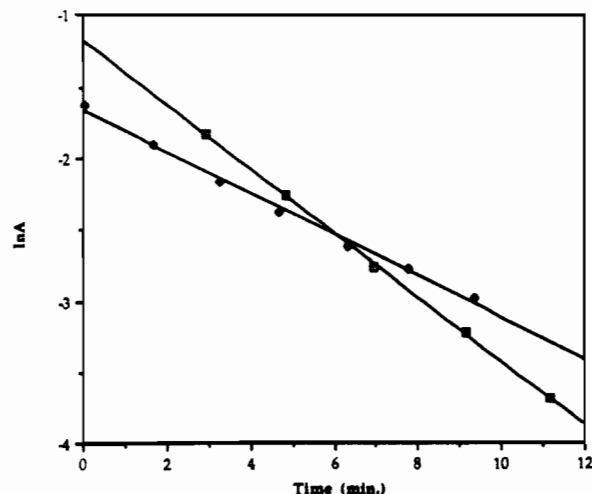


Figure 5. Rate data for CO_2 extrusion from complex 3 in THF at $55.4\text{ }^\circ\text{C}$: \square , argon atmosphere; \blacksquare , CO_2 atmosphere.

tricyclohexylphosphine ligands, the rate of the decarboxylation process was not significantly affected. For example, at 30 and $55.4\text{ }^\circ\text{C}$ in THF the complex $(\text{Cy}_3\text{P})_2\text{CuO}_2\text{CC}(\text{Ph})\text{HCO}_2\text{H}$, 4, undergoes decarboxylation by a first-order process with rate constants of $2.82 \times 10^{-4}\text{ s}^{-1}$ and $3.33 \times 10^{-3}\text{ s}^{-1}$, respectively. On the other hand the decarboxylation process is essentially quenched when carried out in the less polar methylene chloride solvent at $30\text{ }^\circ\text{C}$ as illustrated in Figure 6 (*vide infra*). Related to this

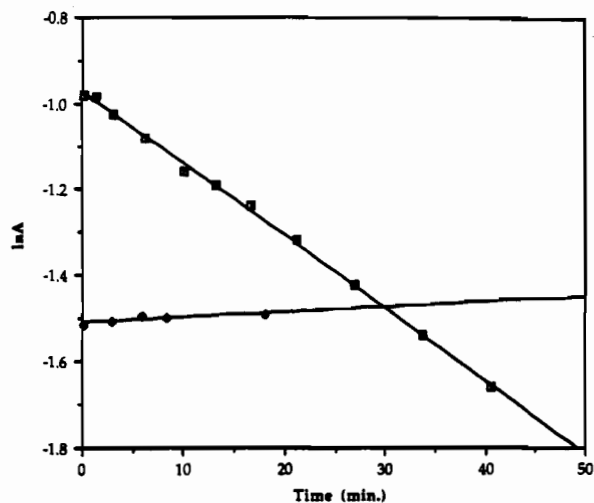
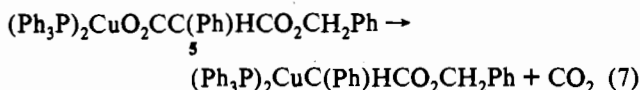


Figure 6. Rate data for CO_2 extrusion from complex 4 at 30 °C: \square , THF solution; \blacksquare , methylene chloride solution.

observation replacement of the acid functionality in complex 3 with the ester moiety (complex 5) greatly accelerates the decarboxylation reaction (eq 7), where a first-order rate constant on the order of 10^{-2} s^{-1} at ambient temperature in THF was noted.



Complexes 3 and 4 are very effective catalysts for the decarboxylation of phenylmalonic acid to phenylacetic acid and carbon dioxide. As shown in Figure 7, the decarboxylation process is first order in [4] and zero order in [acid]. Furthermore, the rate constant for CO_2 extrusion from complex 4 and decarboxylation of phenylmalonic acid are very similar, i.e., k_1 , at 55.4 °C, for CO_2 extrusion is $3.33 \times 10^{-3} \text{ s}^{-1}$ vs $4.07 \times 10^{-3} \text{ s}^{-1}$ for acid decarboxylation. This behavior is consistent with a reaction pathway for the catalytic decarboxylation in the presence of complex 4 where the slow step is the extrusion of CO_2 (see Scheme 1) with phenylacetic acid formation occurring in a subsequent rapid protonation step. A similar observation has been noted for the catalytic decarboxylation of cyanoacetic acid by Cu(I) derivatives.^{22,23} It is of importance to note here that under identical reaction conditions in the absence of Cu(I) reagents, no decarboxylation of the free acid was observed. Evidence for the existence of the Cu-carbon intermediate, $\text{HOCC}(\text{Ph})\text{H}-\text{Cu}(\text{I})$, is manifested by the retardation of the rate of decarboxylation in the presence of CO_2 (or $^{13}\text{CO}_2$), where carbon dioxide reinsertion occurred. Further support for a Cu-carbon intermediate comes as well from the observation that the half-ester derivative, complex 5, undergoes rapid exchange with $^{13}\text{CO}_2$.

The role of hydrogen bonding in the decarboxylation of complex 1 or 4 is apparent. The decarboxylation of the ester complex, 5, where a proton is absent is rapid relative to complex 4 in THF under analogous conditions, although the σ^* values of $-\text{CH}(\text{Ph})\text{COOR}$ and $-\text{CH}(\text{Ph})\text{COOH}$ are nearly identical. On the other hand, in the presence of strong intramolecular hydrogen bonding, a situation which exists in the solid state or in methylene chloride, decarboxylation of complex 4 is greatly retarded. Indeed, in general decarboxylation reactions are extremely medium-sensitive.^{3,24} These observations taken together suggest that

(22) Darensbourg, D. J.; Longridge, E. M.; Atnip, E. V.; Reibenspies, J. H. *Inorg. Chem.* 1992, 31, 3951.

(23) Darensbourg, D. J.; Longridge, E. M.; Holtcamp, M. W.; Klausmeyer, K. K.; Reibenspies, J. H. *J. Am. Chem. Soc.* 1993, 115, 8839.

(24) Grate, J. W.; McGill, R. A.; Hilvert, D. *J. Am. Chem. Soc.* 1993, 115, 8577 and references therein.

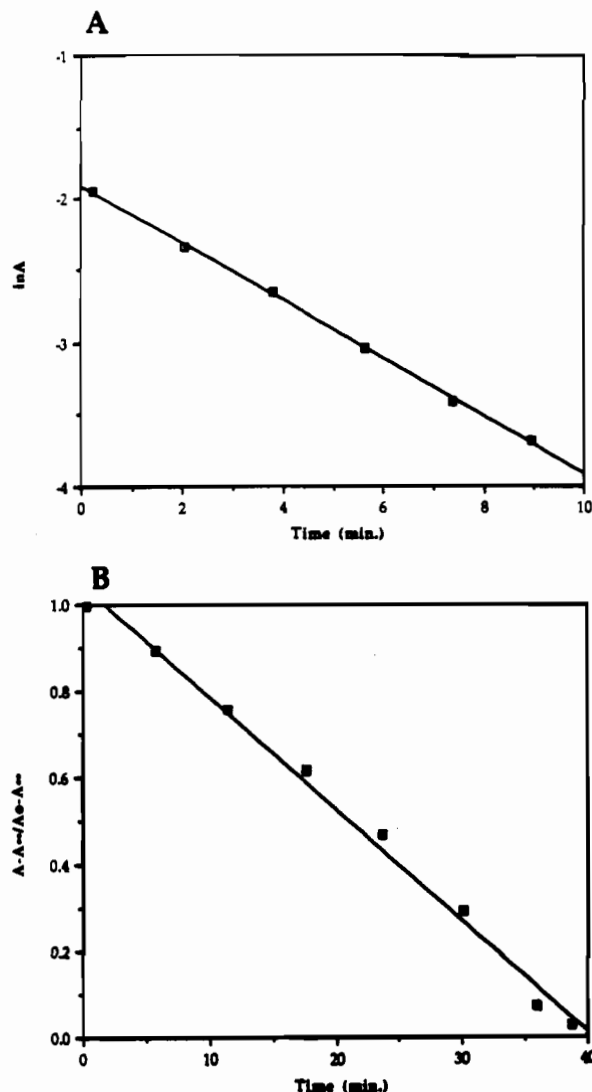


Figure 7. Decarboxylation of phenylmalonic acid in the presence of complex 4: (A) First-order dependence on [4]; (B) zero-order dependence on [acid].

hydrogen bonding to the CO_2 entity which is extruded inhibits the decarboxylation process, whereas intermolecular hydrogen bonding of the distal carboxylic acid function retards the decarboxylation process by effectively reducing the electron-withdrawing ability of the $-\text{CH}(\text{Ph})\text{COOH}$ group by partial deprotonation. Complete deprotonation results in the production of the $-\text{CH}(\text{Ph})\text{CO}_2^-$ group, which is electron-donating, having a σ^* value around -0.10 . In this instance decarboxylation was found not to occur; i.e., $[(\text{Ph}_3\text{P})_2\text{CuO}_2\text{C}(\text{Ph})\text{HCO}_2][\text{Et}_4\text{N}]$ was stable toward decarboxylation. Analogously, the dianion of the free acid is stable toward decarboxylation, even in the molten state.⁴

Current investigations involve the systematic variation of steric and electronic influences about the copper(I) center and in the malonic acid via altering the phosphine ligands and the substituents on the methylene group, respectively. Importantly, we will be studying as well asymmetric decarboxylation of appropriate malonic acid derivatives.⁷

Acknowledgment. Financial support of this research by the National Science Foundation (Grant 91-19737) and the Robert A. Welch Foundation is greatly appreciated.

Supplementary Material Available: Tables providing complete bond lengths, bond angles, and anisotropic thermal parameters for complexes 1 and 2 (6 pages). Ordering information is given on any current masthead page.